Effect of disorder on the Al/GaAs(001) interface

S. K. Donner, K. P. Caffey, and Nicholas Winograd
Department of Chemistry, Pennsylvania State University, University Park, Pennsylvania 16802

(Received 9 February 1989; accepted 18 April 1989)

Distinct differences in the nucleation of Al at room temperature on arsenic-stabilized (2×4)- and $c(4\times4)$-GaAs(001) surfaces grown by molecular-beam expitaxy have been observed with reflection high-energy electron diffraction. The nucleation of Al is found to be dependent upon the amount of disorder on the (2×4)-GaAs(001) surface. Phase diagrams showing the MBE growth parameters required for the preparation of more ordered versus more disordered surfaces of GaAs(001) have been constructed. The presence of disorder has been found to be independent of the rate of cooling of the GaAs substrate to room temperature for Al deposition. Nucleation on the more-disordered (2×4) surface and on the $c(4\times4)$ surface are similar in the direction of twofold periodicity, but differ in the direction of fourfold periodicity. The presence of a strong Al metal adatom–adatom interaction of submonolayer coverages, formerly reported for Al/(2×4)-GaAs(001), may help to explain why the more-ordered (2×4)-reconstructed surface preferentially nucleates fcc Al(110).

I. INTRODUCTION

The techniques currently available to investigate dynamic thin film growth of III–V semiconductors in molecular-beam epitaxy (MBE) continue to be reflection high-energy electron diffraction (RHEED) and electron spectroscopies. Studies of MBE-grown GaAs by scanning tunneling microscopy (STM)[1] have confirmed the missing row model of the arsenic-stabilized (2×4)-GaAs(001) surface (Fig. 1).[2] A one-to-one correspondence between STM results and MBE conditions may not exist, as the STM studies are based on MBE-grown GaAs surfaces that have been capped with an excess of As and removed from the growth chamber.[1] The arsenic cap is then thermally removed before further experiments are performed.[3] However, it has been proposed that the basic (2×4) structural units detected with STM should correspond to the same units under conditions of MBE growth because of electronic stability.[4] The STM pictures of the GaAs(001) surface have also shown that areas of different types of disorder occur.

Under MBE conditions, atomically ordered domains of < 1000 Å are observable with RHEED, whereas domains of < 10 000 Å can be observed with high-resolution RHEED. This allows discrimination between surfaces with long-range areas of one type of symmetry and long-range areas of another.[5] For example, $c(8\times2)/[(4\times2)]$ symmetry has been observed during growth when As/Ga beam-equivalent-pressure ratios are 1:1.[6] The technologically important As-stabilized $(2\times4)/[c(2\times8)]$ surface [hereafter referred to as (2×4)] has been shown to exist over a large area of the growth phase diagram and has also been shown to be disordered over much the same area of the phase diagram.[6]

Disorder on GaAs(001) surfaces has been recognized for some time.[7] The As-stabilized (2×4) and $c(4\times4)$ surfaces generally exhibit more disorder, reflecting the weaker surface binding energy of As. The nature of the disorder on the (2×4) surface has been studied extensively,[8–11] and has until recently only been attributed to the random sequencing of As dimers. However, several different types of one-dimensional order are now being investigated. The observation that hydrogen exposure breaks dimer bonds but that fourfold periodicity persists indicated early on that the dimerization was not causing fourfold periodicity in the [$\bar{1}$10] direction,[11] and that mild random sequencing of the dimers was not sufficient to cause long-range disorder in the fourfold periodicity. Hence, the fourfold periodicity was attributed to surface vacancies.[12] In the presently accepted model of the (2×4) surface, the surface vacancies do occur with a fourfold periodicity.[2] Surface vacancies caused by missing dimers have been attributed to Fermi level instabilities.[13] Rows of missing dimers form in-phase and antiphase boun-

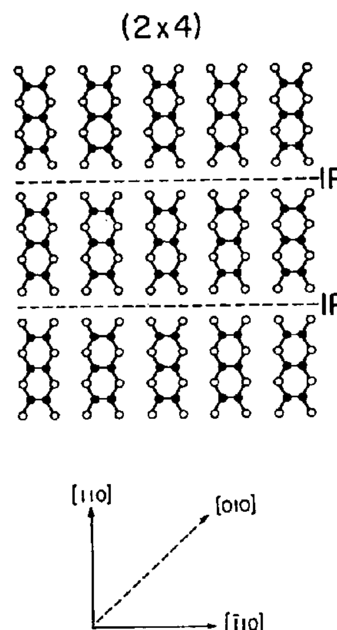

FIG. 1. Currently accepted model of (2×4)-GaAs(001). IP = in-phase boundaries. O Ga. ● As.

 © 1989 American Vacuum Society

daries between units of three dimers. The antiphase boundaries separating (2×4) unit cells form planes in reciprocal space that may intersect the Ewald sphere tangentially, and curvature of the streaks occur.[8,14] The curvature has been most apparent in the half-order streaks in the [010] direction reflecting the dimerization of the surface.

This is important in the present work because the crystallographic relationships between the substrate and Al metal overlayers have been shown to be greatly influenced by the starting substrate morphology as well as its temperature during deposition. The As-rich (2×4)-GaAs(001) surfaces have been extensively investigated because of their device applications. The surface coverages have been determined to be roughly 60%–80% arsenic for this reconstruction.[15–19] The $c(4\times4)$ surface has been shown to be stable over an arsenic coverage of 80% to in excess of 1 monolayer (ML).[17–20] In the limit of bulk single crystallinity, three Al orientations are observed on GaAs(001): (110) with [100] Al parallel to [110] GaAs, (110)R 90° and (001)R 45°. At low temperatures (25–150 °C), low growth rates (200–750 Å/h), and in the thick coverage regime > 2000 Å, the As-rich surfaces yielded the Al(110) orientation while the gallium rich $c(8\times2)$ and (4×6) surfaces and higher deposition rates yielded the (001) orientation of Al.[21–23] High-temperature deposition yields the (110)R 90° structure on all surfaces.[24] In the thin-layer regime from 200–800 Å, As-stabilized surfaces have been shown to promote (110) + (001) three-dimensional nucleation. The (1×1) As surface and $c(4\times4)$ surface also yield the mixed crystal (110) + (001) in this regime.[25] The various structures compensate for the degree of initial lattice mismatch at the interface.

We show in this work that Al deposited onto what we term "more-ordered" (2×4)-GaAs(001) surfaces produces the Al(110) + (001) thin-layer nucleation patterns previously reported for As-stabilized surfaces after 3.5 ML of Al deposition,[24] but that Al deposited onto a "more-disordered" (2×4) surface can produce a different overlayer whose structure reflects the inherent disorder in the (2×4) surface. This Al structure is only observed when the (2×4) surface was more disordered. In the currently accepted definition of a disordered surface, only half-order streaks in the [010] direction extend to the end of the diffraction screen and are curved. No identifiable Al nucleation was observed in the case of an extremely disordered (2×4) surface with a high diffuse background intensity.

II. EXPERIMENT

To ensure a high-quality (001) surface, a 2-μ epitaxial layer of GaAs was grown by MBE prior to *in-situ* metallization. The base pressure of the Riber 2300 MBE growth chamber is 2.0×10^{-11} Torr after bakeout with the liquid nitrogen shrouds filled prior to growth. Silicon-doped GaAs(001) wafers oriented to within ±0.5° were obtained from MA-COM. Substrates were degreased with tricholoroethane, acetone, and methanol and etched with 5:1:1 sulfuric acid:peroxide:water. The native oxide was removed during thermal treatment at 660 °C under an As_4 flux. The background As pressure during Al deposition was less than 1×10^{-9} Torr. Aluminum was deposited at a substrate temperature of 25 °C from an effusion oven heated to 975 °C. The Al growth rate was 0.01 Å s^{-1} as determined by beam-equivalent-pressure calibrations and verified by profilometry measurements. In terms of coverage, this corresponds to a deposition of 0.01 ML s^{-1}, with 1 ML defined with respect to the ideal GaAs (001) surface site density (6.26×10^{14} cm^{-2}). An electron beam of 9.5-keV energy was incident on the sample at a glancing angle of less than 3°. Dynamic RHEED patterns were recorded on video tape for later analysis.

III. RESULTS AND DISCUSSION

A. (2×4) and $c(4\times4)$ surfaces

The room-temperature RHEED patterns for the more-ordered (2×4), more-disordered (2×4), and $c(4\times4)$ reconstructions in the [110], [010], and [$\bar{1}$10] directions are shown in Fig. 2. Most of these pictures have been published elsewhere, and are included here for reference. The most important characteristics, in addition to those that have been previously mentioned, are as follows: (1) the (2×4) pattern reflects the twofold periodicity of As dimers in the [110] direction. (2) We have also found that better quarter-order intensity exists, in general, at room temperature in the [$\bar{1}$10] direction for the more-ordered (2×4) surface, suggesting a higher degree of order. The RHEED pattern of the more-ordered (2×4) surface shown in Fig. 2 (top) show bulk streaks in the 4× direction, which are the same intensity as higher-order streaks. A disordered direction in the surface has been equated with diffraction streaks that are long normal to the shadow edge or broaded in the direction parallel to it, while the more-ordered direction corresponds either to streaks that are short normal to the shadow edge or sharpened in the direction parallel to it.[26] (3) During growth, the middle streak is missing for the more disordered (2×4) reconstruction in the [$\bar{1}$10] direction, and this has been previously attributed to the formation of steps[6] or the presence of disorder during growth.[27] All of the streaks are observed at room temperature, but in the more disordered case, the

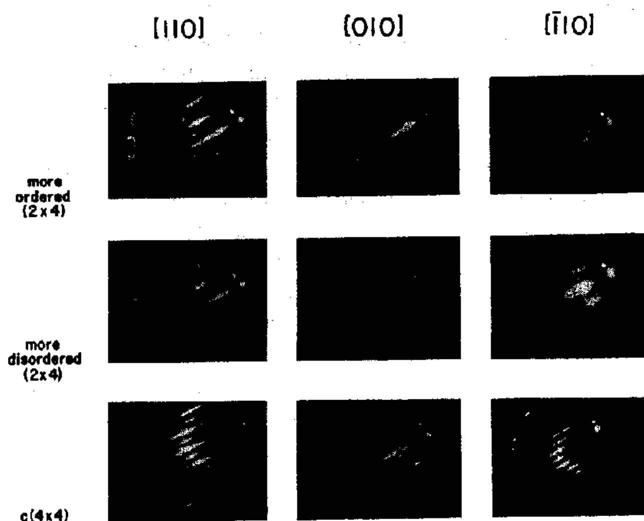

FIG. 2. RHEED patterns at room temperature viewed in the [110], [010], and [$\bar{1}$10] directions.

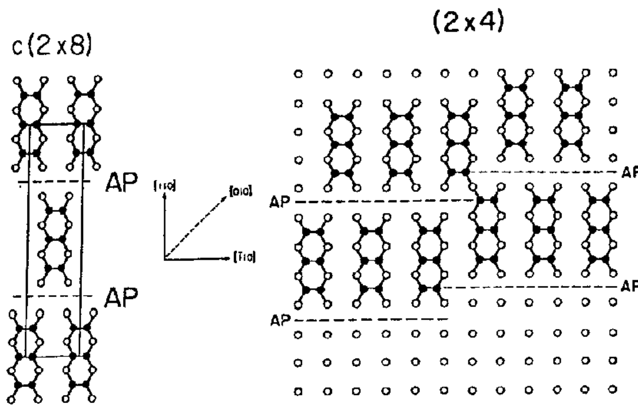

FIG. 3. Types of disorder on GaAs(001) observed by STM. Left, $c(2\times8)$ symmetry; right, closed kink in direction of $4\times$ periodicity. IP = in-phase boundaries, AP = antiphase boundaries. ○ Ga. ● As.

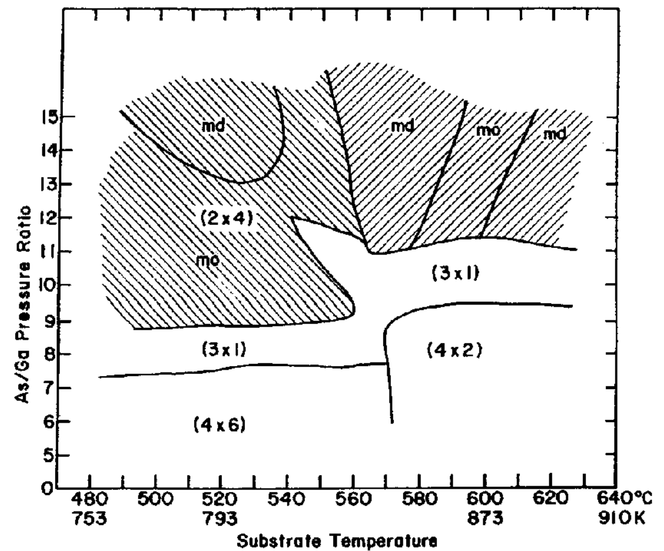

FIG. 4. Surface reconstruction of GaAs(001) versus substrate temperature and the ratio of beam densities measured near the substrate by an ion gauge. Growth rate is 1.5 ML/s. The more-ordered and more-disordered areas are indicated as follows: md = more disordered, mo = more ordered.

bulk streaks are of greater intensity than the higher-order streaks in the [$\bar{1}$10] direction. This represents a form of disorder in the direction of fourfold periodicity.[26] Figure 3 shows models of two types of disorder, randomly sequenced areas of $c(2\times8)$ symmetry and the closed kink, which has been observed wth STM.[1] The closed kink distorts the fourfold periodicity of the surface. It has been shown that areas of $c(2\times8)$ symmetry are randomly sequenced on the GaAs(001) surface, and that they are theoretically lower in energy than areas of (2×4) symmetry by 0.12 eV per unit cell.[2]

The $c(4\times4)$ surface is generated from the (2×4) surface by the chemisorption of excess As or during growth when As/Ga beam-equivalent-pressure ratios are $>20:1$.[20] All of our $c(4\times4)$ surfaces were produced by cooling the (2×4) surface in excess of As. When the As coverage is in excess of ML, an As 3d photoelectron line shape similar to that of amorphous As is observed,[20] reflecting As–As bonding, and results in the observation of the familiar Kikuchi behavior of $c(4\times4)$ surface. This result is consistent with the RHEED data of Fig. 2, seen as intensity patterns, which run diagonally across the screen from the center, and which have been noted elsewhere.[28]

A summary of our observations is presented in Fig. 4 in the form of a phase diagram. The growth rate of this phase diagram is 1.5 ML s^{-1} as calibrated by the RHEED oscillation technique. The more-ordered (2×4) patterns in Fig. 2 were produced from a surface grown in the more-ordered (mo in Fig. 4) areas of the phase diagram; correspondingly, the more-disordered (2×4) pattern shown was produced from a surface grown in any of the more-disordered (md in Fig. 4) (2×4) regions. Growth was performed over a significant range of the phase diagram. The As_4 flux was ceased immediately after growth for every (2×4) surface that was grown at a substrate temperature, Ts < 570 °C. Under higher-temperature growth conditions, the As_4 cell was shuttered before the substrate temperature dropped below 450 °C to prevent the surface from converting to the $c(4\times4)$ reconstruction.

Another more-disordered (2×4) pattern, in addition to the one shown in Fig. 2, is shown in Fig. 5(a). The RHEED pattern in the [010] direction displays only bulk streaks and no curved half-order streaks. However, a 90° rotation of the crystal without changing the flux ratios reveals intense half-order streaks in an equivalent azimuth that are curved. This combination of patterns is observed in the more disordered region of the (2×4) surface phase diagram, and may indicate that some parts of the surface are more disordered than others. By comparison, Fig. 5(b) again shows a more-ordered surface. Half-order streaks are present in the patterns produced from all surfaces; however, the curved streaks from surfaces grown in the more-ordered areas of the phase diagram are less intense than any of those in the more-disordered regions of the phase diagram.

Figure 5(c) shows the RHEED pattern in the [010] direction during the phase transition from the (2×4) surface to $c(4\times4)$ surface. We have observed what may be inter-

FIG. 5. (2×4) RHEED patterns viewed in the [010] direction : (a) only bulk periodicity; (b) only half-order streaks extend to the end of the screen; and (c) quasi-fourfold periodicity on transition from the (2×4) to $c(4\times4)$ surface.

preted as a precursor to the $c(4\times4)$ surface, i.e., an intermediate between the (2×4) and $c(4\times4)$ surfaces. The pattern appears to assume a type of quarter-order periodicity in the [010] direction, as bulk reflections grow more intense. Alternatively, this pattern could be interpreted as an increase in intensity of the half-order streaks in this direction during the transition. Upon adsorption of additional As, the [010] direction may reflect a contraction, then expansion, of the surface to the $c(4\times4)$ value. Changes in the surface during the phase transition have also been noted elsewhere. Scans of the specular beam intensity at an angle of incidence corresponding to the out-of-phase condition (where diffraction is most sensitive to steps) develop the broadened base characteristic of surface step disorder at this transition.[29] The formation of steps may relieve the density changes that occur in phase transitions.[30]

B. Al overlayers

The Al nucleation patterns corresponding to the starting surfaces shown in Fig. 2 are shown in Fig. 6. The Al pattern corresponding to the Al/more-ordered (2×4) surface viewed in the [110] direction is in agreement with earlier experiments,[24] and occurs at roughly 3.5 ML. This pattern is a superposition of two modes of Al growth: Al(110), whose thick-layer coverage diffraction pattern reflects a diamond-shaped pattern, and a portion of the square-arrayed patterns corresponding to Al(001).[31] The twin spots on either side of the specular streak in the Al/more-ordered (2×4) RHEED pattern represent the nucleation of both (001) and (110), with lattice constants of 4.0 and 2.86 Å, respectively. The Al nucleation patterns for the more-ordered (2×4) surface are basically the same when viewed in both the [110] and $[\bar{1}10]$ directions, except that the twinning observed is opposite in intensity in one direction relative to the other, i.e., the pairs of spots rotate in intensity between the two axis. This would

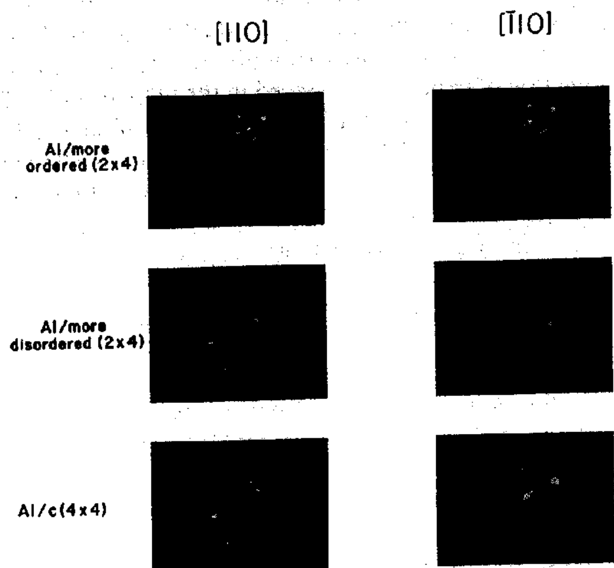

FIG. 6. Aluminum nucleation RHEED patterns: (i) Al/more-ordered (2×4) patterns correspond to 3.5 ML of Al in the [110] direction and 3.8 ML of Al in $[\bar{1}10]$ direction; (ii) Al/more-disordered (2×4) patterns correspond to 2.5 ML of Al; (iii) Al/$c(4\times4)$ patterns correspond to 3.5 ML of Al.

seem to imply that the (001) spots, which are more intense in the [110] direction, signify that Al(001) is forming islands elongated preferentially in this direction and that Al(110) is more predominant when viewed in the $[\bar{1}10]$ direction. Our results at submonolayer coverages also indicte this preferential formation of Al(110) in the $[\bar{1}10]$ direction.[32] The Al(110) crystal predominates on the more-ordered (2×4) surface for thick layers.

The Al(110) spots are missing in the patterns for Al in the [110] direction on the more disordered (2×4) and $c(4\times4)$ surfaces. The nucleation for the (2×4) surface occurs much earlier, at 2.5 ML, and the pattern does not change appreciably with coverage; therefore, since the twinning that would signify the additional formation of Al(110) does not occur, it is obvious that the nucleation in the [110] direction prefers the square-arrayed Al(001). The patterns that are pictured in Fig. 6 for the more-disordered (2×4) surface only become better defined with increasing coverage. A similar nucleation of Al(001) occurs for the $c(4\times4)$ surface in the [110] direction, but at a somewhat higher coverage, 3.5 ML. This may occur as a result of the excess As that is available on the surface to continue the bulk periodicity of the starting substrate.

The Al nucleation patterns for the more-disordered (2×4) and $c(4\times4)$ surfaces are different from each other in the $[\bar{1}10]$ direction. The Al structure on $c(4\times4)$ has been previously identified as (001)R 45°, and our results are consistent with this observation.[22,24] Our results show that the Al nucleation on the more-disordered (2×4) surface is incommensurate in the $[\bar{1}10]$ direction, and a lack of surface basis vectors prevents us from analyzing this structure further. The amount of disorder in this direction may prevent the recognition of a starting substrate, which differs by not more than 1.5% for the Al(110) crystal[23] and not more than 1.3% for the Al(001) crystal rotated 45°.[25] The LEED patterns of these nucleated surfaces may reveal the complete symmetry and rotation.

Nucleation of Al on an extremely disordered (2×4) surface with a high background intensity results in only a highly diffuse pattern with no diffraction spots. Nucleation of a more ordered (2×4) surface such as the one shown in Fig. 2 (top) never fails to result in the Al pattern shown in Fig. 6. The [010]Al patterns are not shown in Fig. 6 as these patterns result in only bulk streaks for the three surfaces during nucleation.

As we previously reported,[32] the regular periodicity of the more-ordered (2×4) surface in the [110] direction creates large open channels between pairs of As dimers, and a (4×1)Al reconstruction forms upon 0.1–0.2 ML of Al deposition. In the $[\bar{1}10]$ direction, Al is also found to undergo a strong metal–metal interaction, which appears to be fostered by long-range channels between pairs of As dimers formed on this stable, well-ordered (2×4) surface, and this may account for the preferential formation of Al(110) on this surface.

IV. CONCLUSION

We have demonstrated the preparation of surfaces that are reasonably well-ordered and of predominantly (2×4)

symmetry. The type and amount of disorder on the (2×4) and $c(4\times4)$ surfaces determines the interaction with Al in the thin-layer regime. The disorder on the $c(4\times4)$ surface from an excess of As and the disorder on the (2×4) surface, possibly produced by random sequencing of dimers and kinks that may distort the fourfold periodicity, determine the ability of Al to form an ordered overlayer on these surfaces. The disorder that has been shown to be significant for Al metal overlayers is long-range and in the direction of 4× periodicity. Auger and XPS data of $c(4\times4)$ and more-disordered (2×4) surfaces may reveal whether Al–As covalent bonding does in fact persist on these surfaces beyond that of the more-ordered (2×4) surface. This may account for the perference of these surfaces to continue the bulk periodicity of the starting substrate and preferentially form Al(001) in the [110] direction.

ACKNOWLEDGMENTS

We would like to express our appreciation to Amoco Research for the depth profiling measurements and also PSU Photographic Services for their assistance. The authors gratefully acknowledge the support of the Office of Naval Research, the National Science Foundation, and the IBM Corporation.

[1]M. D. Pashley, K. W. Haberern, W. Friday, J. M. Woodall, and P. D. Kirchner, Phys. Rev. Lett. **60**, 2176 (1988).
[2]D. J. Chadi, J. Vac. Sci. Technol. A **5**, 834 (1987).
[3]S. P. Kowalczyk, D. L. Miller, J. R. Waldrop, P. G. Newman, and R. W. Grant, J. Vac. Sci. Technol. **19**, 255 (1981).
[4]H. H. Farrell, J. P. Harbison, and L. D. Peterson, J. Vac. Sci. Technol. B **5**, 1482 (1987).
[5]J. H. Neave and B. A. Joyce, J. Cryst. Growth **44**, 387 (1978).
[6]J. M. Van Hove and P. I. Cohen, J. Vac. Sci. Technol. **20**, 726 (1982).
[7]A. Y. Cho, J. Appl. Phys. **42**, 2074 (1971).
[8]P. J. Dobson, J. H. Neave, and B. A. Joyce, Surf. Sci. **119**, L339 (1982).
[9]B. A. Joyce, J. H. Neave, P. J. Dobson, and P. K. Larsen, Phys. Rev. B **29**, 814 (1984).
[10]J. H. Neave, B. A. Joyce, P. J. Dobson, and N. Norton, Appl. Phys. A **31**, 1 (1983).
[11]P. K. Larson and D. J. Chadi, Phys. Rev. B **37**, 8282 (1988).
[12]J. A. Appelbaum, G. A. Baraff, and D. R. Hamann, Phys. Rev. B **14**, 1623 (1976).
[13]A. Y. Cho, J. Appl. Phys. **47**, 2841 (1976).
[14]B. A. Joyce, J. H. Neave, P. J. Dobson, P. K. Larsen, and J. Zhang, J. Vac. Sci. Technol. B **3**, 562 (1985).
[15]P. Drathen, W. Ranke, and K. Jacobi, Surf. Sci. **77**, L162 (1978).
[16]A. J. van Bommel, J. E. Crombeen, and T. G. J. Oirschot, Surf. Sci. **72**, 95 (1978).
[17]R. Z. Bachrach, R. S. Bauer, P. Chiaradia, and G. V. Hansson, J. Vac. Sci. Technol. **18**, 797 (1981).
[18]R. Z. Bachrach, R. S. Bauer, P. Chiaradia, and G. V. Hansson, J. Vac. Sci. Technol. **19**, 335 (1981).
[19]R. Ludeke, T.-C. Chiang, and D. E. Eastman, Physica **117/118B**, 819 (1983).
[20]P. K. Larsen, J. H. Neave, J. F. van der Veen, P. J. Dobson, and B. A. Joyce, Phys. Rev. B **27**, 4966 (1983).
[21]P. M. Petroff, L. C. Feldman, A. Y. Cho, and R. S. Williams, J. Appl. Phys. **52**, 7317 (1981).
[22]R. Ludeke and G. Landgren, J. Vac. Sci. Technol. **19**, 667 (1981).
[23]A. Y. Cho and P. D. Dernier, J. Appl. Phys. **49**, 3328 (1978).
[24]G. Landgren, R. Ludeke, and C. Serrano, J. Cryst. Growth **60**, 393 (1982).
[25]J. Massies and N. T. Linh, Surf. Sci. **114**, 147 (1982).
[26]P. K. Larsen, J. H. Neave, and B. A. Joyce, J. Phys. C **14**, 167 (1981).
[27]J. H. Neave, B. A. Joyce, and P. J. Dobson, Appl. Phys. A **34**, 179 (1984).
[28]P. K. Larsen, G. Meyer-Ehmsen, B. Bolger, and A.-J. Hoeven, J. Vac. Sci. Technol. A **5**, 611 (1987).
[29]C. S. Lent and P. I. Cohen, Phys. Rev. B **33**, 8329 (1986).
[30]J. A. Van Vechten, J. Cryst. Growth, **38**, 139 (1977).
[31]R. Ludeke, L. L. Chang, and L. Esaki, Appl. Phys. Lett. **23**, 201 (1973).
[32]S. K. Donner, J. L. Herman, R. Blumenthal, R. Trehan, E. Furman, and N. Winograd, Appl. Phys. Lett. (submitted).